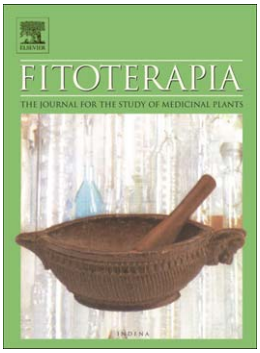

Lignans from the stem bark of *Syringa pinnatifolia*

Guozhu Su, Ruifei Zhang, Xinyao Yang, Ruifeng Bai, Xu Yin, Xiaoli Gao, Li Li, Pengfei Tu, Xingyun Chai

PII: S0367-326X(16)30208-8
DOI: doi: 10.1016/j.fitote.2016.08.011
Reference: FITOTE 3471

To appear in: *Fitoterapia*

Received date: 13 July 2016
Revised date: 18 August 2016
Accepted date: 20 August 2016

Please cite this article as: Guozhu Su, Ruifei Zhang, Xinyao Yang, Ruifeng Bai, Xu Yin, Xiaoli Gao, Li Li, Pengfei Tu, Xingyun Chai, Lignans from the stem bark of *Syringa pinnatifolia*, *Fitoterapia* (2016), doi: 10.1016/j.fitote.2016.08.011

Lignans from the stem bark of *Syringa pinnatifolia*

Guozhu Su [a,b,1], Ruifei Zhang [a,b,1], Xinyao Yang [a,b,1], Ruifeng Bai [a,b], Xu Yin [a,b], Xiaoli Gao [a], Li Li [c], Pengfei Tu [a], and Xingyun Chai [a,*]

[a] Modern Research Center for Traditional Chinese Medicine, Beijing University of Chinese Medicine, Beijing 100029, People's Republic of China

[b] School of Chinese Materia Medica, Beijing University of Chinese Medicine, Beijing 100102, People's Republic of China

[c] Department of Medicinal Chemistry, Institute of Materia Medica, Chinese Academy of Medical Sciences & Peking Union Medical College, Beijing, 100050, People's Republic of China

[*] Corresponding author, Tel/fax: +8610 6428 6350.

E-mail address: xingyunchai@yeah.net (X. Chai).

[1] These authors contributed to the paper equally.

ABSTRACT

Four new lignans, alashinols A–D (**1**–**4**), a new hydrolysis product, alashinols E (**5**), and seven known analogues were isolated from the stem bark of *Syringa pinnatifolia* Hemsl. These new lignans were characterized using 1D and 2D NMR and MS data, and their absolute configurations were determined by experimental and calculated electronic circular dichroism and X-ray diffraction analyses. Alashinol B (**2**) exhibited two conformers that adopted an unusual unit cell packing. Anti-inflammatory evaluation revealed that compounds **1**, **4**, **6**, and **8** showed moderate inhibition against NO production in lipopolysaccharide-induced macrophages RAW 264.7 cells with IC_{50} values range from 43.3–60.9 μM, and **1** decreased the TNF-*α* and IL-6 level in a concentration-dependent manner at 40–160 μM and exhibited considerable neuroprotective effect against the glutamate-induced injury in PC12 cell line. Analogs **3** and **9** showed protective effects against oxygen glucose deprivation/reoxygenation in H9c2 cells.

Keywords:

Syringa pinnatifolia; Lignan; Anti-inflammatory activity; Neuroprotective effect; Antihypoxia effect

1. Introduction

The Chinese endemic species *Syringa pinnatifolia* Hemsl., syn. *S. pinnatifolia* var. *alashanensis* Y.C. Ma & S.Q. Zhou, is a deciduous shrub with pinnately compound leaves mainly found in the Helan Mountains (Ningxia) and Alxa League (Inner Mongolia). Its peeled stem and root, 'Shanchenxiang' in Chinese, serve as one of a representative Mongolian folk medicines against heart and lung diseases. Previous studies revealed that *S. pinnatifolia* contains lignans, sesquiterpenes, and phenylethanoids [1–3]. The essential oils were demonstrated as bioactive ingredients of Shanchenxiang with anti-myocardial ischemic activity [4].

As a part of systematic studies on anti-myocardial ischemic effect and pharmacologically active ingredients of Shanchenxiang [2,5], a phytochemical investigation of its stem bark led to the isolation of four new lignans namely alashinols A–D (**1**–**4**), a new hydrolysis product namely alashinol E (**5**), along with seven known analogues (**6**–**12**). The isolation and structural elucidation of these compounds are described herein in addition to *in vitro* assessments of their anti-inflammatory in RAW264.7 cells, neuroprotective effect in glutamate-induced PC12 cells, and antihypoxia effect in H9c2 cells.

2. Experimental

2.1 General procedures

HR-ESI-MS were recorded using a Shimadzu liquid chromatography-mass spectrometry-ion trap time-of-flight instrument. IR spectra were recorded on a Thermo Nicolet Nexus 470 FT-IR spectrophotometer using KBr pellets. NMR spectra were measured using a Varian-500 spectrometer. Specific rotation (SR) was measured using a Rudolph Autopol IV automatic polarimeter and ECD spectra were acquired using Jasco J-815 spectrometer. Preparative high-performance liquid chromatography (HPLC) was performed using a Waters apparatus equipped with a Shim-pack PREP-ODS (H) (250 × 20 mm, 5 μm) and Shiseido Capcell PAK MG Prep C_{18} (250 × 10 mm, 5 μm). Column chromatography (CC) separations were conducted using silica gel (200–300 mesh, Qingdao Haiyang Chem. Co. Ltd., China), Sephadex LH-20 (GE Healthcare, Sweden), and Li

Chroprep RP-18 (Merck, Germany). Thin layer chromatography (TLC) was performed on pre-coated silica gel GF254 (Qingdao, Haiyang Chem. Co. Ltd, China) and RP-18F254S plates (Merck, Germany).

2.2 Plant material

The stem bark of *S. pinnatifolia*, syn. *S. pinnatifolia* var. *alashanensis* was collected in July 2013 from Alxa League and authenticated by Prof. Chen-Su-Yi-Le (Alashan Mongolian Hospital, Inner Mongolia, China). A voucher specimen (SP201307B) was deposited at the Modern Research Center for Traditional Chinese Medicine, Beijing University of Chinese Medicine.

2.3 Extraction and isolation

Stem bark (1.3 kg) of *S. pinnatifolia* was refluxed with 95 and 80% EtOH (2.5 L, 1.5 h each). After removal of solvent in reduced pressure, the residue (325 g) was subjected to silica gel CC, by a gradient elution of CH_2Cl_2-MeOH (20:1–1:1) to give nine fractions (A–I). Fractions exhibiting characteristic signals within δ_H 3.60–3.90 and 7.50–8.00 ppm in ^{1}H-NMR spectrum were focused on. Specifically, fraction A (48.0 g) was purified by silica gel CC, eluting with petroleum ether-acetone (2:1–0:1) to yield 12 subfractions (A1–A12). A7 (1.0 g) was separated into five fractions (A7a–A7e) by Sephadex LH-20 CC using CH_2Cl_2-MeOH (1:1). A7b (500 mg) was purified by semipreparative C_{18} HPLC (Shim-pack PREP-ODS H 250 × 20 mm, 5 μm; 7 mL/min) using 50% aqueous MeOH as a mobile phase to give **1** (8.7 mg, t_R = 27.9 min) and **6** (30.1 mg, t_R = 60.1 min). Fraction C (31.2 g) was subjected to silica gel CC, eluting with a gradient of CH_2Cl_2-acetone (3:1–1:1) followed by purification on Sephadex LH-20 CC (CH_2Cl_2-MeOH, 1:1) to yield ten fractions (C1–C10). C4 (982 mg) was purified by semipreparative C_{18} HPLC using 50% MeOH as an eluent to yield **4** (5.2 mg, t_R = 17.5 min). C5 (690 mg) was purified by HPLC using 15% aqueous acetonitrile (ACN) to afford **11** (6.0 mg, t_R = 37.3 min), **12** (8.3 mg, t_R = 42.5 min), **8** (5.4 mg, t_R = 44.5 min), and **7** (9.5 mg, t_R = 52 min). Fractions E (10.6 g) and F (8.2 g) were merged and subjected to silica gel CC, eluting with

EtOAc-MeOH (10:1–0:1) to give eight fractions (EF1–EF8) and **2** (70.5 mg). Fraction EF3 (2.5 g) was separated by HPLC using 40% MeOH as an eluent to obtain **10** (6.5 mg, t_R = 20.1 min), **9** (6.3 mg, t_R = 23.5 min), and a mixture that was further purified by HPLC using 16% ACN to yield **3** (6.3 mg, t_R = 26.5 min).

Alashinol A (**1**): white powder; $[\alpha]_D^{25}$ –54.4 (c 0.1, MeOH). UV (MeOH) λ_{max} (log ε): 283 (0.75), 230 (1.90), 206 (4.41) nm. IR (KBr) ν_{max}: 3421, 2918, 1607, 1511, 1453, 1269, 1030 cm^{-1}. ECD (MeOH) λ_{max} ($\Delta\varepsilon$): 239 (–3.30), 274 (–0.51), 293 (+0.43) nm; ^1H and ^{13}C NMR data: see Tables 1 and 2, respectively; HRESIMS *m/z*: 343.1549 $[M + H]^+$ (calcd for $C_{20}H_{23}O_5$ 343.1540).

Alashinol B (**2**): needle crystal; M. p. 174.5–175 ºC; $[\alpha]_D^{25}$ –19.2 (*c* 0.1, MeOH); UV (MeOH) λ_{max} (log ε): 282 (3.90), 228 (4.20), 206 (4.67) nm; IR (KBr) ν_{max} 3423, 2926, 1630, 1384, 1076, 1037 cm^{-1}; ECD (MeOH) λ_{max} ($\Delta\varepsilon$): 209 (+0.45), 230 (+0.50), 241 (–0.95), 282 (–1.01) nm; ^1H and ^{13}C NMR data, see Tables 1 and 2, respectively; HRESIMS *m/z*: 519.1854 $[M – H]^-$ (calcd for 519.1872 $C_{26}H_{31}O_{11}$).

Alashinol C (**3**): white powder; $[\alpha]_D^{25}$ –3.1 (*c* 0.1, MeOH); UV (MeOH) λ_{max} (log ε): 280 (3.86), 227 (4.20), 206 (4.59) nm; IR (KBr) ν_{max}: 3405, 2926, 1516, 1277, 1073, 1038 cm^{-1}; ECD (MeOH) λ_{max} ($\Delta\varepsilon$): 209 (+0.73), 228 (+0.49), 240 (–1.1), 275 (–0.87) nm; ^1H and ^{13}C NMR data, see Tables 1 and 2, respectively; HRESIMS *m/z*: 507.1851 $[M – H]^-$ (calcd for 507.1872 $C_{25}H_{31}O_{11}$).

Alashinol D (**4**): white powder; IR (KBr) ν_{max} 3440, 1632, 1263, 1031 cm^{-1}. UV (MeOH) λ_{max} (log ε) 331 (3.59), 316 (3.56), 283 (4.04), 242 (4.82), 204 (4.63) nm; IR (KBr) ν_{max} 3440, 1632, 1263, 1031 cm^{-1}; ^1H and ^{13}C NMR data, see Tables 1 and 2, respectively; HRESIMS m/z: 355.1202 $[M – H]^-$ (calcd for $C_{20}H_{19}O_6$ 355.1187).

Alashinol E (**5**): white powder; $[\alpha]_D^{25}$ –3.61 (*c* 0.1, MeOH); UV (MeOH) λ_{max} (log ε) 288 (3.67), 214 (4.05) nm; IR (KBr) ν_{max} 3442, 2921, 1636, 1506, 1384, 1037 cm^{-1}; ECD (MeOH) λ_{max} ($\Delta\varepsilon$) 230 (–1.08), 248 (+0.85), 276 (+1.99), 294 (–3.56) nm; ^1H and ^{13}C NMR data, see Tables 1 and 2, respectively; HRESIMS *m/z*: 357.1357 $[M – H]^-$ (calcd for 357.1344 $C_{20}H_{21}O_6$).

Sanshodiol (**6**): white needles; M. p. 148–149 ºC; $[\alpha]_D^{25}$ –14.8 (*c* 0.1, MeOH); UV (MeOH) λ_{max}

(log ε) 284 (3.22), 231 (4.19), 206 (3.94) nm; IR (KBr) ν_{max} 3483, 3423, 2918, 1634, 1513, 1055, 1035 cm^{-1}; ECD (MeOH) λ_{max} ($\Delta\varepsilon$) 206 (+0.90), 236 (+0.74), 245 (–0.55), 292 (–1.42) nm; ^{13}C NMR data, see Table 2, HRESIMS *m/z* 357.1332 $[M - H]^-$ (calcd for 357.1344 $C_{20}H_{21}O_6$).

2.4 Anti-inflammatory assay

RAW 264.7 macrophages were seeded in 96-well plates (2×10^5 cells/well). The cells were pretreated with drugs for 1 h and then incubated with LPS (1 μg/mL) for 24 h. The amount of NO was assessed by determining the nitrite concentration in the cultured RAW 264.7 macrophages supernatants with Griess reagent, and quercetin was used as a positive control, respectively. The absorbance was recorded on a microplate reader at a wavelength of 540 nm. Cells viability were measured by an MTT assay, the absorbance read at 570 nm with an ELISA analyzer [6,7].

2.5 Neuroprotective assay

Rat adrenal pheochromocytoma (PC12) cell lines were seeded in 96-well plates (2×10^5 cells/well). After 24 h, cells were pretreated with drugs for 1 h and then added 50 μL H_2O_2 (1200 μM). Then, after 24 h, cells were incubated with 100 μL MTT solution (0.5 mg/mL) at 37 ºC for another 4 h, the supernatants were removed and residue was dissolved with 150 μL DMSO for each well and subsequently shaked out for 10 min. The absorbance was detected at 570 nm and 630 nm using a microplate reader after the formazan crystals were dissolved. All compounds were dissolved as stock solution in DMSO (final solvent concentration less than 0.2% in any assays) [8].

2.6 TNF-α, IL-6, and quantification by ELISA

RAW264.7 cells were seeded in 96-well plates (2×10^4 cells/well). After incubation for 24 h, the cells were pretreated with **1** for 1 h and then stimulated with LPS (1 μg/mL) for 24 h. The levels of TNF-*α* and IL-6 in the supernatant were measured by ELISA according to the manufacture's protocols.

2.7 Measurement of OGD/re-oxygenation in H9c2 cells

Rat embryonic ventricular H9c2 cardiomyocytes were maintained in Dulbecco's modified eagle's medium (DMEM), supplemented with a 10% fetal bovine serum (FBS),

penicillin/streptomycin, and 4 mM L-glutamine, in a 5% CO_2 incubator at 37 ºC. H9c2 cells were placed in an anaerobic chamber (HERA cell 150, partial oxygen pressure was maintained below 2 mmHg). The medium was replaced with a pre-warmed (37 ºC) glucose-free balanced salt solution (116 mM NaCl, 5.4 mM KCl, 0.8 mM $MgSO_4$, 1.0 mM NaH_2PO_4, 1.8 mM $CaCl_2$, 26.2 mM $NaHCO_3$, 0.025 mM phenol red, and 20 mM sucrose). The solution was bubbled with an anaerobic gas mix (95% N_2, 5% CO_2) for 30 min. Cell cultures subjected to OGD were incubated in the solution at 37 ºC for 1–4 h to produce oxygen deprivation and then re-oxygenated (returned to the normal aerobic environment). Experimental parameters were assayed at 3–24 h following re-oxygenation. Briefly, cells were seeded onto 96-well plates (1.0×10^5 cells/mL) and incubated for 24 h, MTT tetrazolium salt (0.5 mg/mL) was added to each well and incubated in a CO_2 incubator for 2 h at 37 ºC, 100 µL DMSO was then added to dissolve formazan crystals, and the absorbance was recorded at 570 nm. OD values of the treatment group were always normalized to that of the untreated control group [9,10].

3. Results and discussion

Alashinol A (**1**), which was obtained as a white powder, showed a unique *m/z* peak at 343.1549 ($[M + H]^+$, calcd for $C_{20}H_{23}O_5$, 343.1540) by HR-ESI-MS and ^{13}C NMR spectroscopic data, indicating ten degrees of unsaturation. Its infrared (IR) spectrum displayed absorption bands at 3421 and 1511 cm^{-1} for hydroxy and aryl rings, respectively.

The ^1H NMR data (Table 1) indicated that **1** has an ABX coupling system assignable to one 1,3,4-trisubstituted benzene ring [δ_H 6.64 (1H, d, J = 2.0 Hz, H-2), 6.66 (1H, d, J = 8.0 Hz, H-5), 6.49 (1H, dd, J = 2.0, 8.0 Hz, H-6)], two terminal olefinic protons [δ_H 4.79 (1H, s, H-9a), 4.91 (1H, s, H-9b)], two methoxy protons [δ_H 3.73 (3H, s), 3.83 (3H, s)], two aromatic protons [δ_H 6.37 (1H, s, H-2′), δ_H 6.69 (1H, s, H-5′)] assignable to a tetra-substituted benzene ring, and two oxygen connected protons [δ_H 3.55 (1H, dd, J = 2.5, 10.5 Hz, H-9′a) and 3.70 (1H, overlapped, H-9′b)]. The ^{13}C NMR data (Table 2) displayed 20 carbon resonances, including eight quaternary carbons [δ_C 138.3 (C-1), 148.6 (C-3), 145.9 (C-4, 4′), 152.4 (C-8), 128.5 (C-1′), 147.8 (C-3′), 132.3 (C-6′)], and

five tertiary aromatic carbons [δ_C 113.6 (C-2), 115.7 (C-5), 122.5 (C-6), 112.5 (C-2′), 117.0 (C-5′)]. The above assignment suggested **1** to be an arylnaphthalene-type lignan [11], supported by HMBC correlations (Figure 1) from H-5′, H-2, and H-6 to C-7, from H-7 to C-9, C-1′, and C-8′, from H-5 to C-1 and C-3, from H-6 to C-2 and C-4, from H-9 to C-8′, from H-2′ to C-4′ and C-6′, from H-5′ to C-1′ and C-3′, and from H-7′ to C-2′, C-6′, C-9′, and C-8, as well as from 3′-OMe and 3-OMe to C-3′ and C-3, respectively, demonstrating the planar structure of **1**.

The absence of NOESY correlation between H-7 and H-8′ implied a large spatial distance between these two protons, its absolute configuration was defined by comparison of experimental and calculated ECD data. The calculated ECD spectrum of (7*R*, 8′*R*)-**1** showed two negative Cotton effects at 239 and 274 nm and a positive Cotton effect at 293 nm, consistent with experimental data (Figure 2A). Therefore, the absolute configuration of **1** corresponded to (7*R*, 8′*R*), establishing its structure.

The molecular formula of alashinol B (**2**), which formed needle-like crystals, was identified as $C_{26}H_{32}O_{11}$ by HR-ESI-MS and ^{13}C NMR spectroscopic data. Its NMR data (Tables 1 and 2) displayed signals for a glucosyl moiety, which was confirmed by HPLC analysis with authentic sample after enzymatic hydrolysis, two aromatic rings presenting ABX coupling system, one furan ring, one methylenedioxy, one methylene, one oxygen-connected methylene, and one methoxy group, indicating a 7,9′-epoxylignan structure. A comparison of ^{1}H and ^{13}C NMR data with those of **6** revealed their structural similarity, expect for the C-4-bound glucosyl moiety in **2** supported by HMBC correlation from glc-H-1 [δ_H 4.83 (d, J = 7.0 Hz)] to C-4 (δ_C 147.2). The ROESY correlations between H-7 to H-9 and H-7′b of **2** determined its relative configuration [12], which was confirmed as 7*S*, 8*R*, 8′*R* by single-crystal X-ray diffraction analysis (Figure 3).

HR-ESI-MS and ^{13}C NMR spectroscopic data indicated that alashinol C (**3**) matched the molecular formula $C_{25}H_{32}O_{11}$. It exhibited similar UV, IR, and NMR data to alashinol B (**2**), suggesting their structural resemblance. However, a comparison of NMR data (Tables 1 and 2) revealed that 3′,4′-methylenedioxy, 4-glucopyranoside in **2** was replaced by 3′-glucopyranoside,

4′-hydroxy and 4-hydroxy in **3**. This discrepancy were confirmed by HMBC correlation from H-1″ to C-3′ and NOESY correlation of H-1″ and H-2′. The glucose was determined with the same method of **2** after enzymatic hydrolysis. Its relative configuration was assigned by NOESY correlations between H-7 with H-9 and H-7′b. Comparison of the NMR and ECD spectra of **2** and **3** indicated that **3** adopted a (7*S*, 8*R*, 8′*R*) absolute configuration (SI. S35) [12].

Alashinol D (**4**) displayed a HR-ESI-MS signal at *m/z* 355.1202 for $[M - H]^-$, consistent with a molecular ion of the formula $C_{20}H_{20}O_6$ (calcd for $C_{20}H_{19}O_6$: 355.1187) with 11 degrees of unsaturation. Its ^{1}H NMR data (Table 1) showed signals at δ_H 6.88 (d, *J* = 2.0, H-2), 6.93 (d, *J* = 8.0, H-5), and 6.73 (dd, *J* = 2.0, 8.0, H-6) for an 1,2,4-trisubstituted aromatic ring, δ_H 7.25 (s, H-2′) and 6.76 (s, H-5′) for aromatic protons, δ_H 3.98 (s) and 3.84 (s) for two methoxys, δ_H 7.77 (s, H-7′) for one olefinic proton, and δ_H 4.61 (d, *J* = 11.5, H-9a), 4.57 (d, *J* = 11.5, H-9b), and 4.93 (2H, s, H-9′) for four hydroxy methylene protons. Its ^{13}C NMR spectrum (Table 2) exhibited 20 carbon resonances, including 16 olefinic carbons in the low-field region. These assignments, combined with HMBC analysis, suggested that **4** presented an arylnaphthalene-type lignan [11]. HMBC correlations (Figure 1) were observed from H-5′, H-2, H-6, and H-9 to C-7, from H-2′ to C-4′, from H-5′ to C-3′ and C-1′, from H-7′ to C-2′, C-6′, C-9′, and C-8, and from H-9′ to C-8, as well as from 3′-MeO and 3-MeO to C-3′ and C-3, respectively, establishing the final structure.

Alashinol E (**5**) was obtained by refluxing **2** (18.8 mg) with 1 N HCl (1 mL) for 1 h at 90 ºC and purifying the hydrolytic product by a Sephadex LH-20 CC using MeOH as eluent. Its HR-ESI-MS displayed a signal at *m/z* 357.1359 for $[M - H]^-$ corresponding to $C_{20}H_{22}O_6$ (*m/z* calcd for $C_{20}H_{21}O_6$: 357.1344). Its ^{1}H and ^{13}C NMR spectra exhibited similarities to that of (+)-isolariciresinol, except for the replacement of methylenedioxy by MeO-3 and HO-4 in **5** [13]. Its ^{1}H NMR data showed a large $J_{7,8}$ coupling constant of 10.5 Hz, suggesting the opposite orientation of H-7 and H-8. Therefore, C-7 and C-8 adopted a *trans* configuration. NOESY correlation was also observed between H-8′ and H-7, indicating that C-7 and C-8′ was a *cis* configuration [14]. The absolute configuration of **5** was assigned by comparing ECD data with those of (+)-isolariciresinol (**8**),

which displayed opposite Cotton effects (Figure 2B). In addition, its SR data ($[\alpha]_D^{25}$ −3.61, MeOH) was similar to that of *ent*-isolariciresinol ($[\alpha]_D^{25}$ −53.8, MeOH) [15] but opposite to that of (+)-isolariciresinol (**8**) ($[\alpha]_D^{25}$ +34.0, MeOH) on the positive and negative sign of the equations [13], suggesting a (7*R*, 8*S*, 8'*S*) absolute configuration.

Alashinol B (**2**) is of special interest because of its two conformers exhibiting an AABB unit cell packing by X-ray diffraction. These conformers only differ by the benzene ring connected to the methylenedioxy substituent, which is a typical of 7,9′-epoxylignans. Acid hydrolysis of **2** unexpectedly afforded alashinol E (**5**) instead of the aglycone needed for SR data measurement. A process involving acid-mediated furan ring opening, isomerization, and cyclization was proposed for formation of **5** (Scheme 1).

Seven known lignans were isolated with alashinols A–E. Comparison of their NMR spectroscopic, SR or ECD data with previous reports facilitated their structural identification. These lignans included sanshodiol (**6**) [16], burselignan (**7**) [13], (+)-isolariciresinol (**8**) [13], conicaoside (**9**) [17], lariciresinol-4-*O*-*β*-D-glucopyranoside (**10**) [18], (–)-olivil (**11**) [19], and dysosmarol (**12**) [20]. With the ^{13}C NMR data, the configuration of **6** was determined by SR and ECD data analyses for the first time [16] (SI. S35).

These lignans were tested *in vitro* for anti-inflammatory, neuroprotective effect, and antihypoxia effect. The results showed that **1**, **4**, **6**, and **8** inhibited the lipopolysaccharide (LPS)-induced NO production in RAW 264.7 cells with their IC_{50} values of 60.9, 43.3, 49.8, and 46.0 μM, respectively, compared with a positive control quercetin (IC_{50} = 15.3 μM). Moreover, compound **1** exhibited inhibition on the production of inflammatory mediators TNF-*α* and IL-6, especially, it significantly suppressed the increase of IL-6 level in a concentration dependent manner at 40–160 μM (Figure 4).

Compounds **3** and **9** at 40 μM significantly increased the cell viability with 80.7 ± 5.6% and 79.8 ± 0.7% of the control value (100%), respectively, compared with the model group with 67.0 ± 4.2% of the control value against oxygen glucose deprivation/re-oxygenation injury in H9c2 cardiomyocytes.

The present finding not only enriches the lignan study, but also brings potential reference to clarifying bioactive ingredient of Shanchenxiang with anti-myocardial ischemic function.

4. *X-ray Crystal Data for Alashinol B (**2**)*

Needle crystal, $C_{26}H_{32}O_{11}$, M = 520.52, monoclinic, crystal size 0.45 × 0.20 × 0.15 mm^3, space group $P2_1$ (no. 4), a = 25.7104 (6) Å, b = 10.28363 (18) Å, c = 19.2514 (4) Å, α = 90.00, β = 111.621 (2), γ = 90.00, V = 473.89 (17) $Å^3$, Z = 8, μ(Cu Kα) = 0.9064, D_{calcd} = 1.461 mg/mm^3, F (000) = 2208, 39079 reflections measured, 16696 unique (R_{int} = 0.0281) which were used in all calculation, final R indexes for I > 2σ (I), R_1 = 0.0377, wR_2 = 0.0995, R indexes for all data R_1 = 0.0520, wR_2 = 0. 1112. Flack parameter = –0.05 (7). Crystallographic data for **2** have been deposited with the Cambridge Crystallographic Data Centre (deposition number: CCDC 1054351).

5. *Acid and enzymatic hydrolysis of **2***

In acidic conditions, the phenolic glycoside **2** was hydrolyzed to give the free phenol **A**. Further hydrolysis of the tetrahydrofuran ring in **A** was facilitated by the para-phenol group, affording the para-quinone methide intermediate **B**. The reactive intermediate **B** could be intercepted by the nearby electron-rich aromatic ring, thus forming the observed podophyllotoxin type product **5** through intermediate **C** (Scheme 1).

Compound **2** (1.26 mg) was which dissolved in DMSO treated with 0.3 mg of cellulose (Beijing Biotech Biochemistry Technical Co.) in citric acid buffer solution (PH 4.5, 60 mL). The mixture was stirred at 40 ºC for 12 h, and then extracted with an equal amount of EtOAc. The EtOAc layer was evaporated under reduced pressure to obtain the alashinol **2a** which was identified by co-TLC confirmation with compound **6**. The *β*-D-glucopyranoside was dissolved in anhydrous pyridine (1 mL), and then L-cysteine methyl ester hydrochloride (5 mg) was added to the solution. The mixture was heated at 60 ºC for 1 h, and *O*-tolyl isothiocyanate (3 mg) was subsequently added. Followed by heated at 60 ºC for another 1 h. Finally, the reaction mixture was analyzed by C_{18} HPLC (Aglient Eclipse XDB 4.6 × 250 mm, 5 μm) using 25% ACN at 0.8 mL/min, and the detection wavelength was set at 254 nm. The result indicated the retention time was identified for 16.58 min.

Acknowledgments

This paper is financially supported by grants from the National Natural Science Foundation of China (Nos. 81473426, 81303309). The authors express their thanks to Prof. Chen-Su-Yi-Le (Alashan Mongolian Hospital) for his collection and authentication of plant material.

Appendix A. Supplementary data

The MS, NMR, and ECD spectra of **1**–**6** and X-ray crystallographic data of **2** are available in the online version.

Reference

[1] G. Su, J. Chen, Y. Cao, R. Bai, S. Chen, P. Tu, et al., Phytochemical and pharmacological progress on peeled stem of *Syringa pinnatifolia*, a Mongolian folk medicine. China J. Chin. Mater. Med. 40 (2015) 4333–4338.

[2] G. Su, R. Bai, X. Yu, Y. Cao, X. Yin, P. Tu, et al., Noralashinol A, a new norlignan from the stem barks of *Syringa pinnatifolia.* Nat. Prod. Res. DOI: 10.1080/14786419.2016.1146886.

[3] S. Chen, G. Su, R. Bai, X. Yin, Y. Cao, P. Tu, et al., Iridoids from the stem barks of *Syringa pinnatifolia.* China J. Chin. Mater. Med. 41 (2016) 1246–1250.

[4] Y. Yan, W. O, X. Zhao, X. Ye, C. Zhang, J. Hao, et al., Effect of essential oil of *Syringa pinnatifolia* Hemsl. var. *alashanensis* on ischemia of myocardium, hypoxia and platelet aggregation. J. Ethnopharmacol. 131 (2010) 248–255.

[5] Y. Cao, J. Wang, G. Su, Y. Wu, R. Bai, Q. Zhang, et al., Anti-myocardial ischemia effect of *Syringa pinnatifolia* Hemsl. by inhibiting expression of cyclooxygenase-1 and -2 in myocardial tissues of mice. J. Ethnopharmacol. 187 (2016) 259–268.

[6] D. Chen, Z. Xu, X. Chai, K. Zeng, Y. Jia, D. Bi, et al., Nine 2-(2-phenylethyl) chromone derivative from the resinous wood of *Aquilaria sinensis* and their inhibition of LPS-induced NO production in RAW 264.7 cells. Eur. J. Org. Chem. 27 (2012) 5389–5397.

[7] N. Li, J.Y. Zhang, K.W. Zeng, L. Zhang, Y.Y. Che, P.F. Tu, Anti-inflammatory homoisoflavonoids from the tuberous roots of *Ophiopogon japonicus*. Fitoterapia 83 (2012) 1042–

1045.

[8] L.Y. Wang, J. Wu, Z. Yang, X.J. Wang, Y. Fu, H.M. Liu, et al., (*M*)- and (*P*)-bicelaphanol A, dimeric trinorditerpenes with promising neuroprotective activity from *Celastrus orbiculatus*. J. Nat. Prod. 76 (2013) 745–749.

[9] K.L. Zheng, Z.Q. Sheng, Y.F. Li, H.H. Lu, Salidroside inhibits oxygen glucose deprivation (OGD)/re-oxygenation-induced H9c2 cell necrosis through activating of Akt-Nrf2 signaling. Biochem. Bioph. Res. Co. 451 (2014) 79–85.

[10] J.J. Shao, Y. Peng, L.M. Wang, J.K. Wang, X. Chen, Activation of sphk1 by k6pc-5 inhibits oxygen-glucose deprivation/reoxygenation-induced myocardial cell death. DNA Cell Biol. 34 (2015) 1–8.

[11] S.A.S. Da Silva, A.L. Souto, M. De Fatima Agra, E.V.L. Da Cunha, J.M. Barbosa Filho, M.S. Da Silva, et al., A new arylnaphthalene type lignan from *Cordia rufescens* A. DC. (Boraginaceae). Arkivoc 6 (2004) 54–58.

[12] H. Nishiwaki, M. Kumamoto, Y. Shuto, S. Yamauchi, Stereoselective syntheses of all stereoisomers of lariciresinol and their plant growth inhibitory activities. J. Agric. Food Chem. 59 (2011) 13089–13095.

[13] A. Jutiviboonsuk, H. Zhang, G.T. Tan, C. Ma, H.N. Van, N.M. Cuong, et al., Bioactive constituents from roots of *Bursera tonkinensis*. Phytochemistry 66 (2005) 2745–2751.

[14] J.M. Fang, C.K. Lee, Y.S. Cheng, Lignans from leaves of *Juniperus chinensis*. Phytochemistry 31 (1992) 3659–3661.

[15] J.G. Urones, J.D.P. Teresa, I.S. Marcos, D.D. Martin, Ent-isolariciresinil in *Reseda suffruticosa*. Phytochemistry 5 (1987) 1540–1541.

[16] F. Abe, S. Yahara, K. Kubo, G. Nonaka, H. Okabe, I. Nishioka, Studies on *Xanthoxylum* spp. II. Constituents of the bark of *Xanthoxylum piperitum* DC. Chem. Pharm. Bull. 22 (1974) 2650–2655.

[17] J. Zhou, X. Zhou, C. Liang, X. Su, B. Li, Y. Qing, et al., Chemical constituents of *Dendrobium officinale*. Chin. Tradit. Herbal Drugs 9 (2015) 1292–1295.

[18] M. Sugiyama, M. Kikuchi, Characterization of lariciresinol glucosides from *Osmanthus asiaticus*. Heterocycles 36 (1993) 117–121.

[19] M.L.B. Pinheiro, A.F. Rocha, M.A.N. Femandes, Lignanas de *Strychnos guianensis* (Aublet) Mart. Quim. Nova. 27 (2004) 188–192.

[20] R.W. Jiang, J.R. Zhou, P.M. Hon, S.L. Li, Y. Zhou, L.L. Li, et al., Lignans from *Dysosma versipellis* with inhibitory effects on prostate cancer cell lines. J. Nat. Prod. 70 (2007) 283–286.

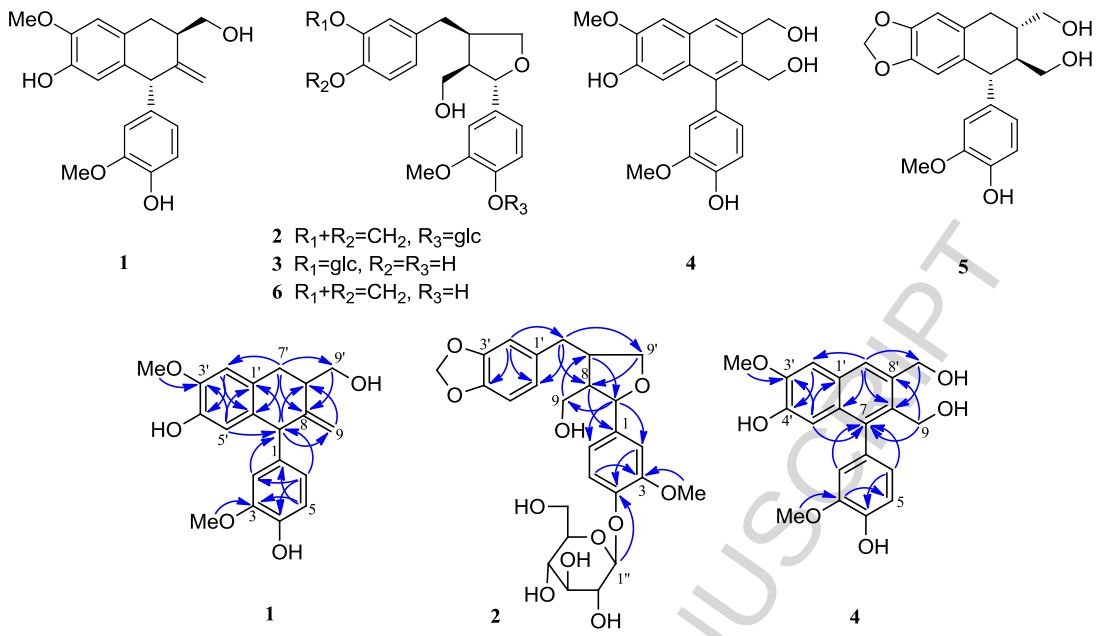

Figure 1. Structures of **1**–**6** and key HMBC correlations of **1**, **2**, and **4**.

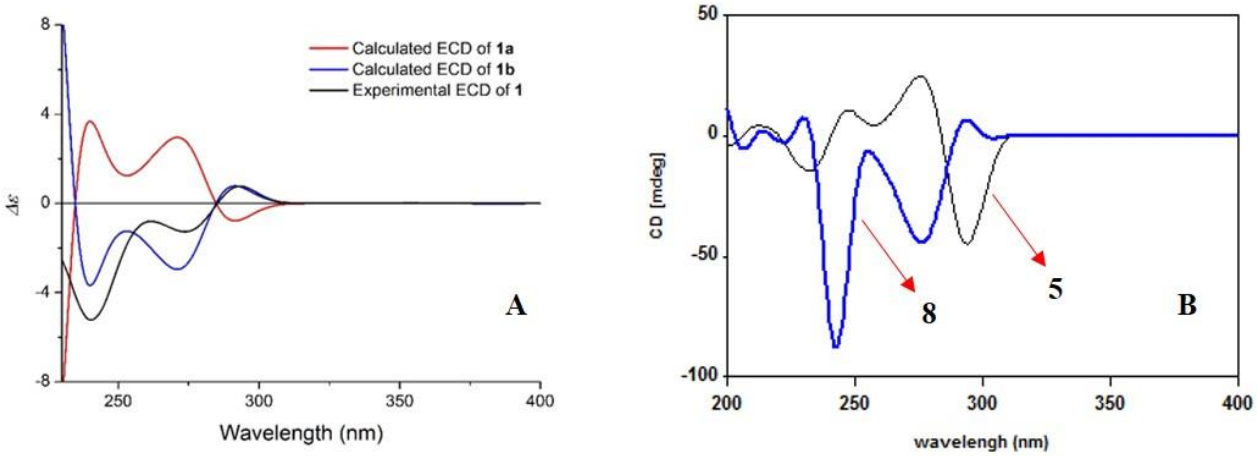

Figure 2. Calculated ECD spectra of **1** (7*R*, 8'*R*), **1a** (7*S*, 8'*S*), and **1b** (7*R*, 8'*R*) (**A**), and ECD spectra of **5** and **8** (**B**)

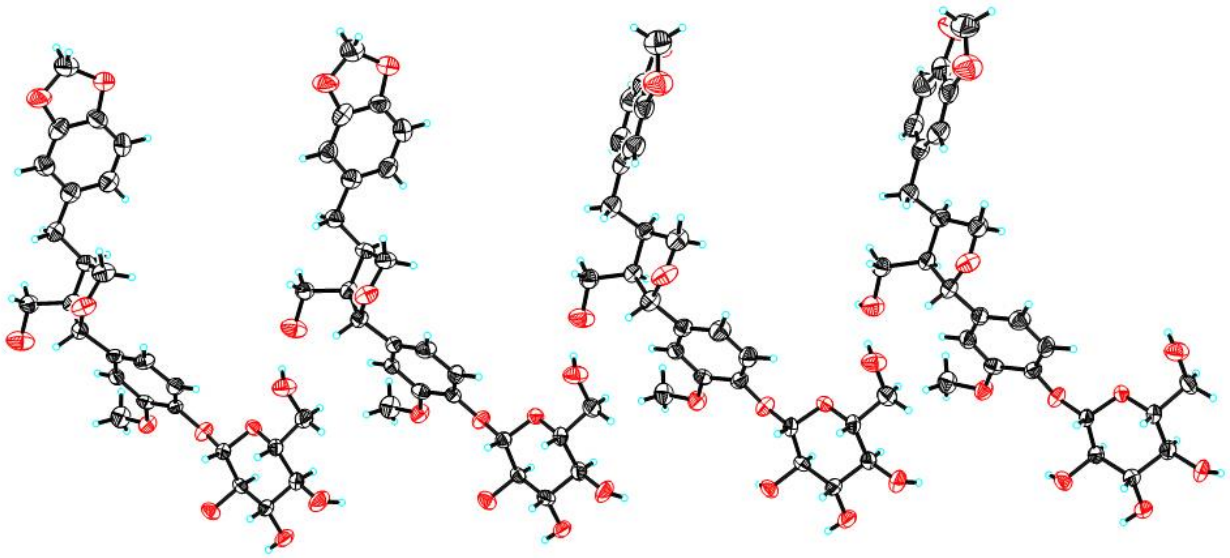

Figure 3. X-ray ORTEP drawing of compound **2**.

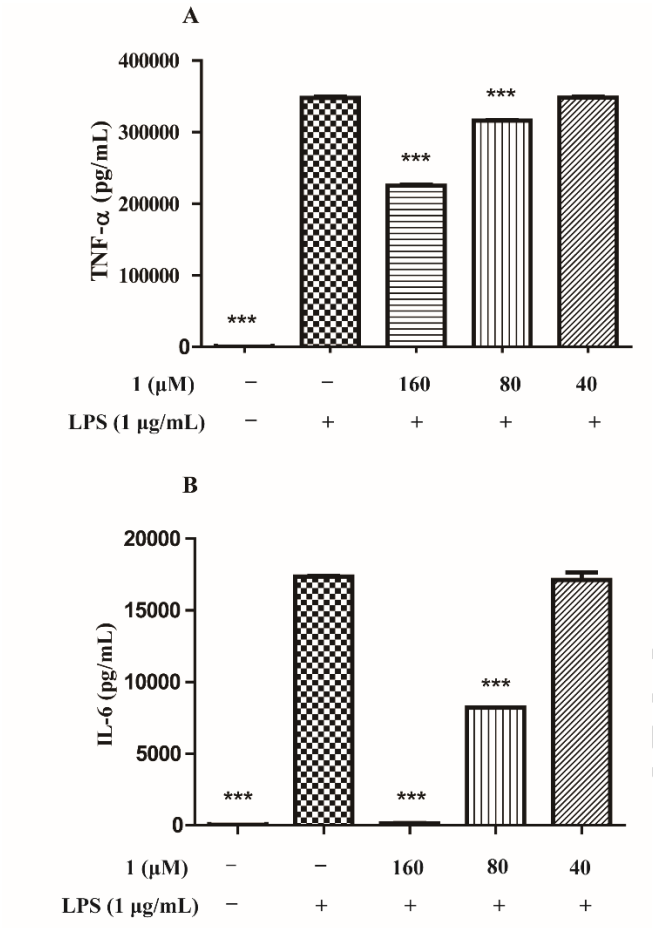

Figure 4. Effects of compound **1** on LPS-induced expression of TNF-*α* and IL-6. RAW264.7 cells were pretreated with various concentrations of compound **1** for 1 h and then stimulated with LPS (1 μg/mL) for 24 h. Data was obtained from three independent experiments. $^{***}P < 0.001$ *vs* LPS group.

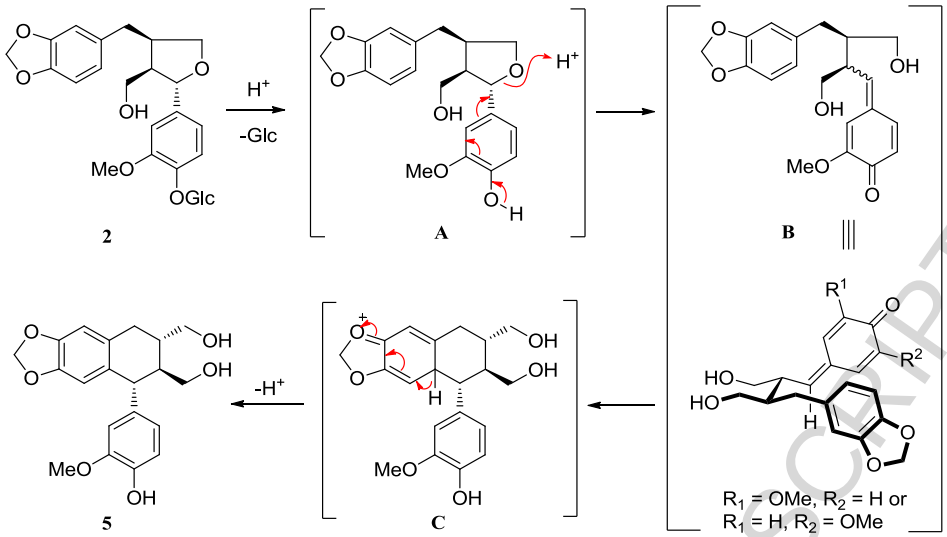

Scheme 1. Plausible sequential reaction that transforms **2** into **5** at 90 ºC in 1 N HCl (1 mL)

Table 1. ^{1}H NMR (500 MHz in CD_3OD) of **1**–**5**, δ in ppm and J in Hz

NO.	**1**	**2**	**3**	**4**	**5**
2	6.64, d (2.0)	6.92, br s	6.89, br s	6.88, d (2.0)	6.67, d (1.5)
5	6.66, d (8.0)	7.08, d (8.0)	6.75, overlapped	6.93, d (8.0)	6.74, d (8.0)
6	6.49, dd (2.0, 8.0)	6.81, d (8.0)	6.75, overlapped	6.73, dd (2.0, 8.0)	6.60, dd (2.0, 8.0)
7	4.52, s	4.75, overlapped	4.74, d (7.0)		3.82, d (10.5)
8		2.27, m	2.34, m		1.76, m
9a	4.79, s	3.75, m	3.80, m	4.61, d (11.5)	3.64, m
9b	4.91, s	3.59, m	3.61, dd (6.5, 11.5)	4.57, d (11.5)	3.38, dd (4.0, 11.0)
2'	6.69, s	6.64, br s	7.05, br s	7.25, s	6.57, br s
5'	6.37, s	6.66, d (7.5)	6.76, overlapped	6.76, s	6.13, br s
6'		6.58, d (7.5)	6.76, overlapped		
7'a	2.56, dd (8.5, 15.5)	2.82, m	2.89, dd (5.0, 13.5)	7.77, s	2.76, br s
7'b	3.04, dd (5.5, 15.5)	2.42, m	2.49, dd (2.0, 13.5)		2.74, br s
8'	2.65, m	2.60, m	2.73, m		1.98, m
9'a	3.55, dd (2.5, 10.5)	3.92, m	3.99, dd (6.5, 8.5)	4.93, s	3.67, m
9′b	3.70, overlapped	3.64, m	3.68, m		3.60, m
MeO-3	3.73, s	3.79, s	3.83, s	3. 84, s	3.77, s
MeO-3'	3.83, s			3.98, s	
OCH_2O		5.83, br s			5.78, br s
1"		4.83, d (7.0)	4.73, d (7.0)		
2"		3.45, m	3.46, m		
3"		3.44, m	3.46, m		
4"		3.35, m	3.38, m		
5"		3.35, m	3.39, m		
6"a		3.82, d (12.5)	3.71, d (11.5)		
6"b		3.64, m	3.70, m		

[a]Chemical shifts (ppm) referred to CD_3OD (δ_H 3.33)

Table 2. ^{13}C NMR (125 MHz in CD_3OD) of **1**–**5**, δ in ppm.

NO.	**1**	**2**	**3**	**4**	**5**	**6**
1	138.3, C	139.4, C	135.8, C	132.1, C	138.3, C	135.7, C
2	113.6, CH	111.3, CH	110.6, CH	115.3, CH	113.7, CH	110.7, CH
3	148.6, C	150.7, C	149.0, C	148.8, C	149.1, C	149.0, C
4	145.9, C	147.2, C	147.0, C	146.8, C	146.1, C	147.3, C
5	115.7, CH	117.8, CH	116.0, CH	116.0, CH	116.1, CH	116.0, CH
6	122.5, CH	119.5, CH	119.8, CH	124.2, CH	123.1, CH	119.8, CH
7	53.4, CH	83.8, CH	84.1, CH	140.0, C	48.4, CH	84.1, CH
8	152.4, C	53.9, CH	53.9, CH	133.4, C	47.9, CH	54.0, CH
9	108.9, CH_2	60.5, CH_2	60.5, CH_2	60.7, CH_2	62.3, CH_2	60.4, CH_2
1'	128.5, C	135.8, C	133.7, C	130.1, C	131.0, C	135.9, C
2'	112.5, CH	109.9, CH	119.0, CH	107.4, CH	108.8, CH	110.0, CH
3'	147.8, C	147.2, C	146.7, C	150.3, C	147.1, C	147.1, C
4'	145.9, C	149.1, C	146.5, C	147.8, C	147.1, C	149.2, C
5'	117.0, CH	109.1, CH	117.0, CH	110.8, CH	110.3, CH	109.1, CH
6'	132.3, C	122.6, CH	124.9, CH	130.3, C	134.8, C	122.7, CH
7'	35.0, CH_2	33.7, CH_2	33.4, CH_2	127.2, CH	33.9, CH_2	33.8, CH_2
8'	41.9, CH	43.7, CH	43.7, CH	136.8, C	39.9, CH	43.8, CH_2
9'	65.0, CH_2	73.5, CH_2	73.5, CH_2	64.5, CH_2	65.8, CH_2	73.4, CH_2
MeO-3	56.3, CH_3		56.4, CH_3	56.4, CH_3	56.4, CH_3	56.4, CH_3
MeO-3'	56.4, CH_3	56.7, CH_3		56.2, CH_3		
OCH_2O		102.1, CH_2			101.8, CH_2	102.1, CH_2
1"		102.8, CH	104.2, CH			
2"		74.8, CH	74.9, CH			
3"		77.7, CH	77.6, CH			
4"		71.3, CH	71.3, CH			
5"		78.1, CH	78.3, CH			
6"		62.5, CH_2	62.4, CH_2			

[a]Chemical shifts (ppm) referred to CD_3OD (δ_C 49.0)

Graphical Abstract

Lignans from the stem bark of *Syringa pinnatifolia*

Guozhu Su [a,b,1], Ruifei Zhang [a,b,1], Xinyao Yang [a,b,1], Xu Yin [a,b], Ruifeng Bai [a,b], Xiaoli Gao [a], Li Li [c], Pengfei Tu [a], and Xingyun Chai [a,*]

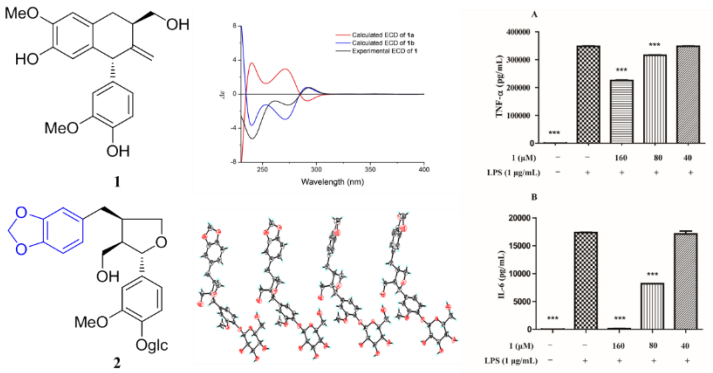

* Corresponding author, Tel/fax: +8610 6428 6350.

E-mail address: xingyunchai@yeah.net (X. Chai).

[1] These authors contributed to the paper equally.